Acta Crystallographica Section F
Structural Biology and Crystallization Communications
ISSN 1744-3091

Purification, crystallization and data collection of *Pectobacterium chrysanthemi* AcsD, a type A siderophore synthetase

Stephen A. McMahon,[a] Muse Oke,[a] Huanting Liu,[a] Kenneth A. Johnson,[a] Lester Carter,[a] Nadia Kadi,[b] Malcolm F. White,[a] Gregory L. Challis[b] and James H. Naismith[a]*

[a]Scottish Structural Proteomics Facility and Centre for Biomolecular Sciences, The University, St Andrews, Fife KY16 9ST, Scotland, and [b]Department of Chemistry, University of Warwick, Coventry CV4 7AL, England

Correspondence e-mail: naismith@st-and.ac.uk

Received 1 September 2008
Accepted 6 October 2008

AcsD, a type A siderophore synthetase with a molecular weight of 71 140 Da from *Pectobacterium chrysanthemi*, has been expressed, purified and crystallized at 293 K. The protein crystallized in the primitive orthorhombic space group $P2_12_12_1$, with unit-cell parameters $a = 80.3$, $b = 95.7$, $c = 161.1$ Å, $\alpha = \beta = \gamma = 90^\circ$. Systematic absences were consistent with space group $P2_12_12_1$. A complete data set has been collected to 2.25 Å resolution on BM14 at the ESRF. Consideration of the likely solvent content suggested that the asymmetric unit contained two molecules. Gel-filtration experiments indicated that the protein was a dimer, although self-rotation analyses did not detect a convincing twofold symmetry axis in the asymmetric unit. The protein has no convincing sequence match to any known structure and thus solution is likely to require experimental phasing.

1. Introduction

Iron is an essential cofactor for both microorganisms and pathogens. In microorganisms it is required for ATP biosynthesis, whilst in pathogens it is often essential in establishing virulence. Unfortunately, iron is not freely available in the environment or higher eukaryotes as it is either insoluble (Fe^{3+}) or already being utilized by other proteins (Bullen & Griffiths, 1999). As a consequence of this, iron assimilation is a significant challenge for both saprophytic microorganisms and invading pathogens. To overcome this problem, many pathogenic microorganisms synthesize and excrete iron-sequestering molecules called siderophores (Wandersman & Delepelaire, 2004). Siderophores scavenge ferric iron from the host and are readsorbed into the cell *via* a selective membrane-associated ATP transport system, where Fe^{3+} is then reduced to Fe^{2+} for release from the siderophore complex, storage and utilization (Koster, 2001).

Two biosynthetic routes exist for siderophores that yield structurally distinct molecules. Most polypeptide-based siderophores, for example pyoverdins, are biosynthesized *via* the well characterized nonribosomal peptide synthetase (NRPS) multienzyme family (Challis & Naismith, 2004), whereas many nonpolypeptide siderophores are biosynthesized *via* the much less well understood NRPS-independent siderophore (NIS) pathway (Challis, 2005). The *Escherichia coli* siderophore aerobactin was the first siderophore identified to be assembled by an NIS pathway (De Lorenzo *et al.*, 1986). Over the last 10 y, several more NIS pathways for biosynthesis of a structurally diverse group of siderophores have been discovered. A superfamily of enzymes termed the NIS synthetases is common to all these pathways. NIS synthetases have been subdivided into A, B and C subfamilies according to their predicted substrate specificities. The NIS synthetase superfamily encompasses over 80 proteins from more than 40 bacterial species (Challis, 2005). Very recently, the first biochemical studies of AsbA, a type A NIS synthetase, and DesD, a type C NIS synthetase, have been reported (Oves-Costales *et al.*,

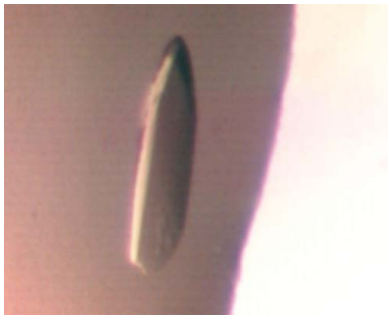

2007; Kadi *et al.*, 2007), confirming the predicted substrate specificities of these enzymes (Challis, 2005).

Pectobacterium chrysanthemi is a Gram-negative plant pathogen that is known to cause soft rot in various hosts. Two siderophores, chrysobactin and achromobactin, are required for full virulence of this pathogen. While chrysobactin is assembled by an NRPS-dependent pathway, achromobactin biosynthesis is NRPS-independent and involves type A, B and C NIS synthetases (Franza *et al.*, 2005). The gene cluster that directs achromobactin production comprises eight genes, five of which (*acsF*, *acsE*, *acsD*, *acsC* and *acsA*) are proposed to be required for biosynthesis. Its expression is regulated by iron availability *via* direct interaction of iron with the ferric uptake regulatory protein Fur (Franza *et al.*, 2005).

AcsD (MW 71 140 Da, pI 6.7) has been classified as a type A siderophore synthetase on the basis of sequence comparisons (Challis, 2005). According to the model for NIS synthetase substrate specificity, it is likely that AcsD catalyses the condensation of one of the prochiral carboxyl groups of citric acid with either the hydroxyl group of ethanolamine, the hydroxyl group of D- or L-serine or the N4-amino group of L-2,4-diaminobutyric acid (Fig. 1; Challis, 2005). However, the order of the steps in achromobactin biosynthesis remains to be clarified and it is possible that AcsA catalyzes the condensation of the δ-carboxyl group of α-ketoglutarate with the amino group of ethanolamine or the 2-amino group of 2,4-diaminobutyric acid prior to AcsD-catalysed condensation of the product of one of these reactions with citric acid.

The achromobactin-biosynthetic pathway offers potential targets for the design of new drugs against *P. chrysanthemi* and other pathogens containing related siderophore-biosynthetic pathways. As yet, there are no known three-dimensional structures of NIS synthetases. As part of our program on deciphering NIS siderophore biosynthetic pathways, we have cloned, expressed, purified and crystallized AcsD.

2. Materials and methods

2.1. Cloning, expression and purification

The gene encoding AcsD was amplified from cosmid pL9G1 (Franza *et al.*, 2005) and cloned into the pET151/D-TOPO vector (Invitrogen). The expressed construct contains an N-terminal tobacco etch virus protease-cleavable site between the protein and a hexahistidine tag. The resulting plasmid was used to transform *E. coli* BL21 (DE3) (Novagen). 10 l of cells was grown in tryptone phosphate broth with ampicillin (final concentration 100 µg ml^{-1}) at 310 K. When the cells reached an A_{600} of 0.6, 0.4 m*M* isopropyl β-D-1-thiogalactopyranoside (IPTG) was added and the temperature was lowered to 288 K. High temperatures led to insoluble overexpression. After a further 18 h incubation period, cells were harvested by centrifugation at 2500*g* and 277 K for 30 min and resuspended in phosphate-buffered saline (PBS). The mixture was centrifuged as before and cell pellets were stored at 193 K.

Cell pellets were resuspended in lysis buffer (50 m*M* sodium phosphate pH 7.5, 500 m*M* NaCl, 30 m*M* imidazole, 10% glycerol, 1 mg ml^{-1} lysozyme) with protease inhibitors and lysed on ice using a Constant Systems cell disruptor at 207 MPa. The crude lysate was clarified by centrifugation (15 000*g*, 30 min, 277 K) and passed through a 0.22 µm filter. The cell-free extract was loaded onto a Nickel Sepharose 6 Fast Flow column (GE Healthcare) and the column was washed extensively with lysis buffer containing 50 m*M* imidazole before elution of AcsD in lysis buffer containing 500 m*M* imidazole. We found that AcsD precipitates if left in imidazole-containing buffer for any significant time. Fractions containing AcsD were immediately passed through a desalting (HiPrep 26/10) column (GE Healthcare), eluting with 50 m*M* Tris, 500 m*M* NaCl, 10% glycerol pH 7.5. The His tag was removed by incubation with TEV protease (mass ratio 1:50) overnight for 15 h at 293 K. The protease and uncleaved protein were removed by passage through a column in

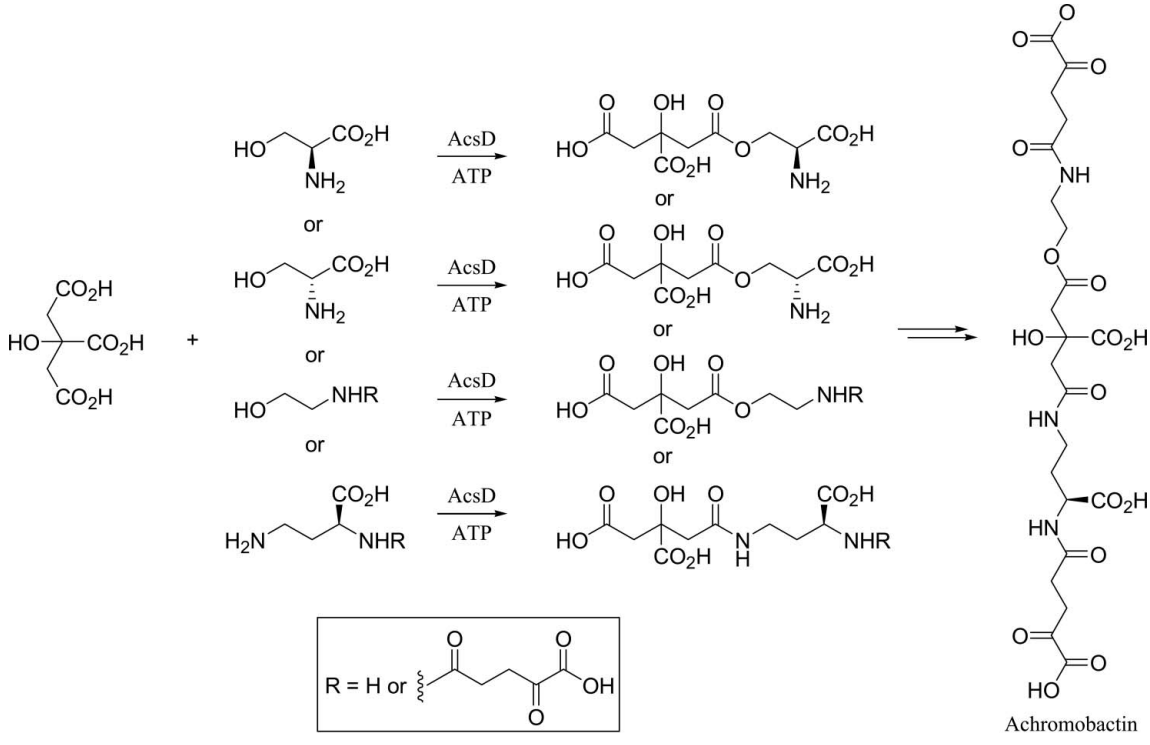

Figure 1
Possible reactions hypothesized to be catalyzed by AcsD.

50 m*M* Tris, 500 m*M* NaCl, 10% glycerol pH 7.5 containing Nickel Sepharose 6 Fast Flow medium. AcsD was further purified by gel filtration on an S-200 column (GE Healthcare) in 10 m*M* Tris, 150 m*M* NaCl, 10% glycerol pH 7.5. The purified protein (Fig. 2), which contains an additional N-terminal alanine residue when compared with the native protein, was characterized by SDS–PAGE and mass spectrometry before being concentrated to 5 mg ml^{-1} in gel-filtration buffer for crystallization.

2.2. Crystallization

Initial crystallization conditions for AcsD were identified using screening by sitting-drop vapour diffusion with a variety of commercial crystallization kits (The Classics and JCSG crystallization screens from Qiagen) and one custom PEG-based screen. Preliminary trials with these precipitants screened three different final protein concentrations. These were 0.1 µl AcsD (2.5 mg ml^{-1}) mixed with 0.1 µl precipitant, 0.2 µl AcsD (2.5 mg ml^{-1}) mixed with 0.1 µl precipitant and 0.1 µl AcsD (5 mg ml^{-1}) mixed with 0.1 µl precipitant. Drops were set up at 293 K and were prepared using a nanodrop crystallization robot (Cartesian HoneyBee) as a part of a Hamilton–Thermo Rhombix system in Greiner Bio-One sitting-drop square-well plates with 100 µl of precipitant per reservoir. Small crystals (0.1 × 0.05 × 0.05 mm) were observed in various conditions throughout the screens, but the best crystals, as judged morphologically, were obtained using 0.1 *M* Tris–HCl pH 8.5 and 1.0 *M* sodium tartrate. Systematic optimization of this condition was performed in conventional sitting-drop plates by mixing 1 µl AcsD (2.6 mg ml^{-1}) and 1 µl precipitant and equilibrating over 500 µl precipitant at 293 K. This resulted in slightly larger crystals (0.2 × 0.1 × 0.1 mm) that grew to full size in one week (Fig. 2) from 0.1 *M* Tris–HCl pH 8.5 and 1.5 *M* sodium tartrate.

2.3. X-ray data collection

The crystals of AcsD were soaked for 5–10 s in a cryoprotectant solution which consisted of 1.5 *M* sodium tartrate, 0.1 *M* Tris–HCl pH 8.5 and 20% glycerol. The soaked crystal was mounted in a cryo-loop (Hampton) and placed into a stream of nitrogen at 100 K. Diffraction data were collected on a MAR 225 CCD on BM14 at the European Synchrotron Radiation Facility (ESRF), Grenoble. The incident X-ray beam had a wavelength of 0.976 Å. 200 frames were recorded with a crystal-to-detector distance of 220 mm as non-overlapping 0.5° oscillations with 60 s exposure per image. A typical image is shown in Fig. 3. The data were integrated and reduced with the program *XDS* (Kabsch, 1993). Initial indexing showed the crystals to be primitive orthorhombic, with unit-cell parameters $a = 80.3$, $b = 95.7$, $c = 161.1$ Å, $\alpha = 90$, $\beta = 90$, $\gamma = 90°$. A study of the systematic absences revealed absences consistent with space group $P2_12_12_1$ and this was supported by the *CCP*4 program *POINTLESS* (Collaborative Computational Project, Number 4, 1994). Data-collection statistics are given in Table 1.

Table 1
Crystal data and data-collection statistics.

Values in parentheses are for the highest resolution shell.

Wavelength (Å)	0.976
Resolution (Å)	50.0–2.25 (2.38–2.25)
Space group	$P2_12_12_1$
Temperature (K)	100
Detector	MAR 225 CCD
Unit-cell parameters (Å, °)	$a = 80.3$, $b = 95.7$, $c = 161.1$, $\alpha = 90$, $\beta = 90$, $\gamma = 90$
V_M, dimer (Å^3 Da^{-1})	2.17
Solvent content, dimer (%)	43
Unique reflections	58435 (9054)
Total reflections	178029 (27763)
Average $I/\sigma(I)$	11.1 (2.9)
Average redundancy	3.0 (3.0)
Data completeness (%)	98.2 (99.6)
R_{merge}†	0.098 (0.40)

† $R_{merge} = \sum_{hkl}\sum_i |I_i(hkl) - \langle I(hkl)\rangle| / \sum_{hkl}\sum_i I_i(hkl)$, where $I(hkl)$ is the measured diffraction intensity and the summation includes all observations.

3. Results and discussion

Calculation of the Matthews coefficient (V_M = 2.17 Å^3 Da^{-1}) suggested the presence of two molecules of AcsD in the asymmetric unit and a solvent content of 43.3%. A monomer or trimer in the asymmetric unit gave Matthews coefficients of 4.3 and 1.45 Å^3 Da^{-1} with solvent contents of 72% and 15%, respectively. When compared with protein standards of known molecular weight, the elution profile of AcsD from S-200 gel-filtration columns is consistent with the weight of a dimer (~150 kDa; data not shown). This evidence would suggest that there are two molecules in the asymmetric unit. Self-rotation analysis does not identify a threefold rotation axis, but there is no strong peak on the $\kappa = 180°$ section to suggest the presence of a twofold axis. There is no significant sequence match between AcsD and any structure deposited in the Protein Data Bank (PDB). We will therefore have to rely on experimental phasing strategies to solve the structure. We have expressed and crystallized selenomethionine-derivatized AcsD using the procedures outlined above, modified only

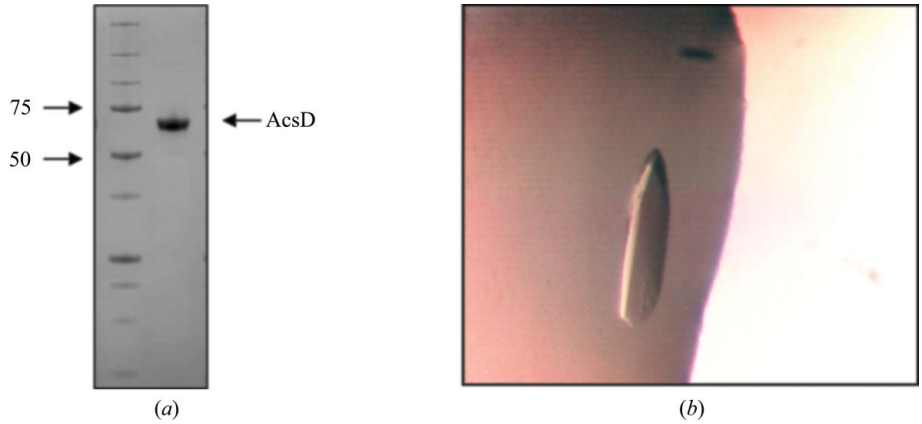

Figure 2
(*a*) SDS–PAGE showing purified AcsD and (*b*) a typical crystal.

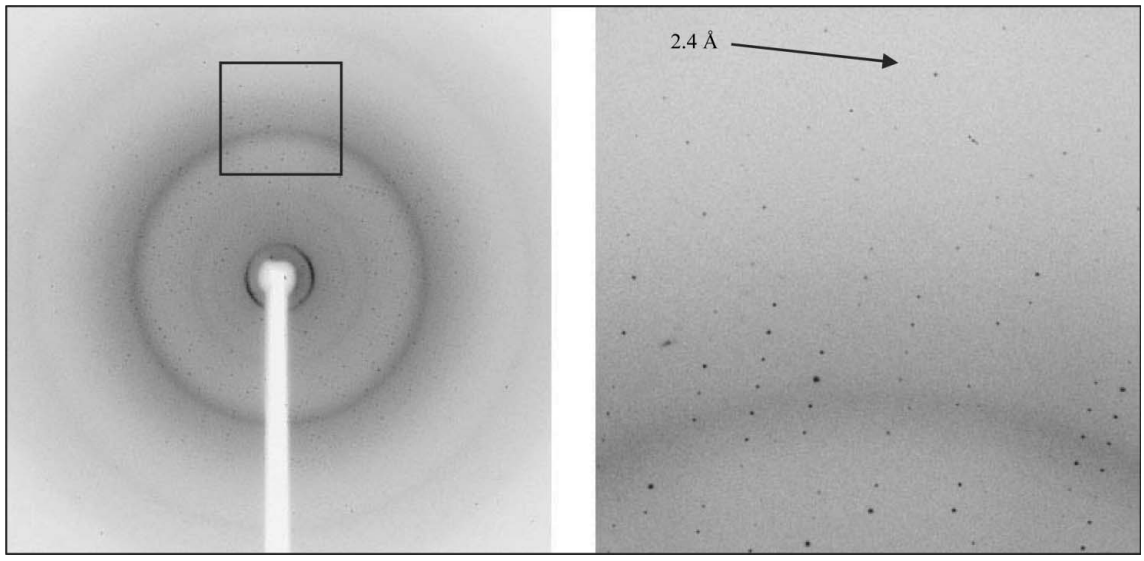

Figure 3
Diffraction pattern of AcsD. Data were collected on BM14 at the ESRF.

to prevent methionine biosynthesis. Although the selenomethionine-derivatized AcsD crystals are small, we expect to be able to improve their quality and then utilize the anomalous signal from Se to solve the structure by multi-wavelength anomalous dispersion methods shortly.

The structure of AcsD will provide an insight into the molecular mechanism of citrate recognition and whether the enzyme discriminates between the two prochiral carboxymethyl groups of citrate. Additionally, a structure will facilitate the design of inhibitors of AcsD and homologues, *e.g.* AsbA, which catalyses the ATP-dependent condensation of citric acid with spermidine as the first committed step in the biosynthesis of the anthrax 'stealth siderophore' petrobactin (Oves-Costales *et al.*, 2007). Such inhibitors may form the basis for the development of new antibiotics. The structure of AcsD may also aid in the elucidation of the reaction it catalyses in achromobactin biosynthesis. Based on the available data, AcsD could catalyse the ATP-dependent condensation of one of the prochiral carboxyl groups of citric acid with one of several different diamine, amino alcohol, amido amine or amido alcohol substrates (Fig. 1).

NK and GLC thank Professor Dominique Expert for the gift of cosmid pL9G1. Mark Dorward and Michal Zawadzki are thanked for valuable technical support. The protein was targeted as part of the Scottish Structural Proteomics Facility (SSPF), which is funded by the Scottish Higher Education Funding Council (SHEFC) and the Biotechnology and Biological Sciences Research Council (BBSRC), UK.

References

Bullen, J. J. & Griffiths, E. (1999). *Iron and Infection*, 2nd ed., pp. 327–368. New York: John Wiley & Sons.
Challis, G. L. (2005). *Chembiochem*, **6**, 601–611.
Challis, G. L. & Naismith, J. H. (2004). *Curr. Opin. Struct. Biol.* **14**, 748–756.
Collaborative Computational Project, Number 4 (1994). *Acta Cryst.* D**50**, 760–763.
De Lorenzo, V., Bindereif, A., Paw, B. H. & Nielands, J. B. (1986). *J. Bacteriol.* **165**, 570–578.
Franza, T., Mahe, B. & Expert, D. (2005). *Mol. Microbiol.* **55**, 261–275.
Kabsch, W. (1993). *J. Appl. Cryst.* **26**, 795–800.
Kadi, N., Oves-Costales, D., Barona-Gomez, F. & Challis, G. L. (2007). *Nature Chem. Biol.* **3**, 652–656.
Koster, W. (2001). *Res. Microbiol.* **152**, 291–301.
Oves-Costales, D., Kadi, N., Fogg, M. J., Song, L., Wilson, K. S. & Challis, G. L. (2007). *J. Am. Chem. Soc.* **129**, 8416–8417.
Wandersman, C. & Delepelaire, P. (2004). *Annu. Rev. Microbiol.* **58**, 611–647.